



POTSDAM-INSTITUT FÜR
KLIMAFOLGENFORSCHUNG

Originally published as:

Mbouna, S. G. N., Banerjee, T., [Schöll, E.](#), Yamapi, R. (2023): Effect of fractional derivatives on amplitude chimeras and symmetry-breaking death states in networks of limit-cycle oscillators. - Chaos, 33, 6, 063137.

DOI: <https://doi.org/10.1063/5.0144713>

RESEARCH ARTICLE | JUNE 12 2023

Effect of fractional derivatives on amplitude chimeras and symmetry-breaking death states in networks of limit-cycle oscillators

Special Collection: [Chimera states: from theory and experiments to technology and living systems](#)

S. G. Ngueuteu Mbouna ; Tanmoy Banerjee ; Eckehard Schöll  ; René Yamapi 



Chaos 33, 063137 (2023)

<https://doi.org/10.1063/5.0144713>

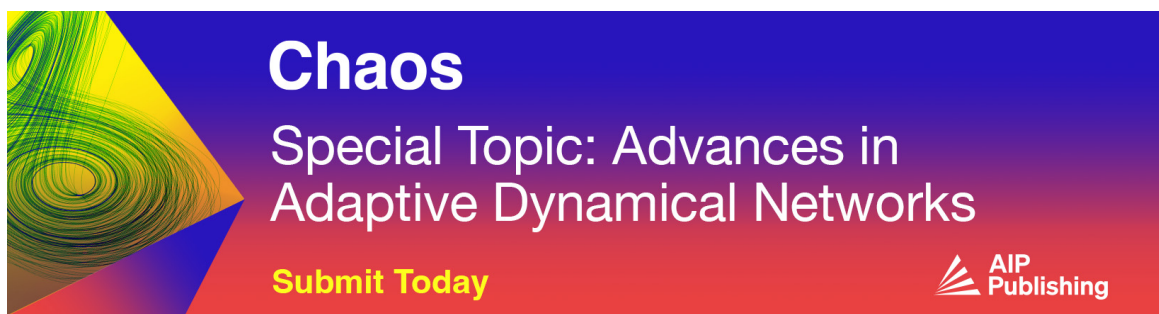


View
Online




Export
Citation

CrossMark



Chaos
Special Topic: Advances in
Adaptive Dynamical Networks
Submit Today



Effect of fractional derivatives on amplitude chimeras and symmetry-breaking death states in networks of limit-cycle oscillators

Cite as: Chaos 33, 063137 (2023); doi: 10.1063/5.0144713

Submitted: 31 January 2023 · Accepted: 22 May 2023 ·

Published Online: 12 June 2023



View Online



Export Citation



CrossMark

S. G. Ngueuteu Mbouna,¹  Tanmoy Banerjee,²  Eckehard Schöll,^{3,4,5,a)}  and René Yamapi⁶ 

AFFILIATIONS

¹Laboratory of Modeling and Simulation in Engineering, Biomimetics and Prototypes, Faculty of Science, University of Yaoundé I, P.O. Box 812, Yaoundé, Cameroon

²Chaos and Complex Systems Research Laboratory, Department of Physics, University of Burdwan, Burdwan 713 104, India

³Institut für Theoretische Physik, Technische Universität Berlin, Hardenbergstraße 36, 10623 Berlin, Germany

⁴Potsdam Institute for Climate Impact Research, Telegrafenberg A 31, 14473 Potsdam, Germany

⁵Bernstein Center for Computational Neuroscience Berlin, Humboldt-Universität, 10115 Berlin, Germany

⁶Fundamental Physics Laboratory, Department of Physics, Faculty of Science, University of Douala, P.O. Box 24 157, Douala, Cameroon

Note: This paper is part of the Focus Issue on Chimera states: from theory and experiments to technology and living systems.

^{a)}Author to whom correspondence should be addressed: schoell@physik.tu-berlin.de

ABSTRACT

We study networks of coupled oscillators whose local dynamics are governed by the fractional-order versions of the paradigmatic van der Pol and Rayleigh oscillators. We show that the networks exhibit diverse amplitude chimeras and oscillation death patterns. The occurrence of amplitude chimeras in a network of van der Pol oscillators is observed for the first time. A form of amplitude chimera, namely, “damped amplitude chimera” is observed and characterized, where the size of the incoherent region(s) increases continuously in the course of time, and the oscillations of drifting units are damped continuously until they are quenched to steady state. It is found that as the order of the fractional derivative decreases, the lifetime of classical amplitude chimeras increases, and there is a critical point at which there is a transition to damped amplitude chimeras. Overall, a decrease in the order of fractional derivatives reduces the propensity to synchronization and promotes oscillation death phenomena including solitary oscillation death and chimera death patterns that were unobserved in networks of integer-order oscillators. This effect of the fractional derivatives is verified by the stability analysis based on the properties of the master stability function of some collective dynamical states calculated from the block-diagonalized variational equations of the coupled systems. The present study generalizes the results of our recently studied network of fractional-order Stuart–Landau oscillators.

Published under an exclusive license by AIP Publishing. <https://doi.org/10.1063/5.0144713>

Coupled oscillator models have been used as a paradigm for the mathematical description of real-life processes that manifest as macroscopic collective dynamics of many interacting objects. Due to the coupling, the local dynamics might be reorganized in such a way that the oscillations synchronize^{1–4} or diverse oscillatory patterns emerge spontaneously in a coupled system. The chimera pattern is a peculiar form of partial synchronization characterized by spatially separated domains of coherent and incoherent behavior.^{5–8} Also due to the coupling, the local dynamics might be stabilized to a unique steady state (a situation termed as amplitude death^{9,10}) or to different symmetry-breaking steady

states (oscillation death^{9,10}). Chimera and oscillation death are symmetry-breaking phenomena, as they appear in systems of symmetrically coupled identical oscillators. In a recent work,¹¹ we found that fractional derivatives impact amplitude chimeras and induce the occurrence of diverse other symmetry-breaking states in a network of fractional-order Stuart–Landau oscillators. In the present work, we generalize the results of this previous work by considering two networks of fractional-order counterparts of two other limit-cycle oscillators, namely, the van der Pol and Rayleigh oscillators. Although amplitude chimeras were already observed in networks of Rayleigh oscillators, it is only in the present work

that their occurrence in a network of van der Pol oscillators is highlighted for the first time.

I. INTRODUCTION

At all scales (cosmic, macroscopic, and microscopic), the objects around us are in perpetual motion that very often demonstrates a certain degree of repetition. So, our surroundings are full of objects that produce rhythms, generally in the form of oscillating processes. Usually these objects are not isolated from their environment, but interact with their counterparts. A multitude of phenomena in natural and man-made systems can be explained as macroscopic collective dynamics of many interacting objects—the simplest and most famous of these collective dynamics is synchronization, which can be basically defined as the entrainment of rhythms of interacting elements,¹ or as the adjustment of the time scales of oscillations due to interaction between the oscillatory processes.² Over the last few decades, the study of synchronization phenomena has attracted a lot of attention in the international scientific community in general, and in the nonlinear science community in particular,^{1–4} due to the fact that apart from pure academic interest, the study of synchronization phenomena is relevant in explaining rhythms in natural and technological dynamical systems.

Among the large variety of synchronization phenomena discovered in the last decades, there is a peculiar form of partial synchronization called the chimera state that has been the subject of an intense activity in the field of coupled nonlinear systems.^{7,8} In a chimera state, the coupled system splits up spontaneously in two subsystems with synchronous and asynchronous elements, respectively. In a broad sense, in a chimera state, coherent and incoherent behaviors coexist in the coupled system in spatially separated domains. Surprisingly, the chimera state arises in networks of symmetrically coupled identical elements⁷ as a consequence of spontaneous symmetry-breaking. Another symmetry-breaking phenomenon that has also received a great deal of interest during the last decades is oscillation death (OD). In an oscillation death state, the coupling induces the quenching of oscillations and gives rise to the birth of stable inhomogeneous steady states.^{9,10,12} It has been found that chimera states and oscillation death appear usually in the same coupled systems. For example, the two phenomena have been observed in coupled systems of the Stuart–Landau model,^{12,13} van der Pol model,^{14,15} Rayleigh model,¹⁶ FitzHugh–Nagumo model (without cross-coupling terms,¹⁷ and with cross-coupling terms¹⁸), and Rosenzweig–MacArthur model.¹⁹ An important connection between these two symmetry-breaking states is the chimera death state,¹³ which generalizes the chimera state feature to oscillation death states such that separated regions of spatially coherent and incoherent steady states coexist in the coupled system. The OD state is a collective state where the dynamics of the different oscillators is stabilized at an inhomogeneous steady state, whereas the chimera death state is a particular form of OD state where a group or some groups of adjacent oscillators populating the same steady state (coherent steady states) appear(s) spontaneously while the other oscillators are distributed randomly over different steady states (incoherent steady states).

For their dynamical analysis, the basic features of the aforementioned systems are more often described by sets of first-order differential equations. For example, let t be the time, and \mathbf{x} the vector of dynamical variables, then, the system is given by $\dot{\mathbf{x}}(t) = \mathbf{f}(t, \mathbf{x}(t))$, where the dot over the variables denotes the first-order derivative with respect to time and $\mathbf{f}(\cdot)$ is a vector function. Now, to accurately account for experimental data when describing many real-life systems, the first-order derivatives with respect to time should be generalized by real-number-order derivatives also known as fractional-order derivatives.²⁰ Thus, the system should be described by the following fractional-order differential equation: $D_t^{\mathbf{a}} \mathbf{x}(t) = \mathbf{f}(t, \mathbf{x}(t))$, where \mathbf{a} is a vector whose dimension is the same as \mathbf{x} ; D_t^{α} is the fractional derivative operator that, applied to a given dynamical variable, denotes its derivative of order α with respect to time t , where α is a component of \mathbf{a} and $\alpha \in \mathbb{R}_+^*$. Fractional-order differential equations have been used to describe successfully various phenomena such as viscoelasticity,^{21,22} anomalous diffusion and transport,²³ dielectric losses,^{24–26} eddy current and hysteresis losses in magnetic coils,^{25,27} processes in biology and bioengineering (power-law adaptation in the firing activity of neurons, anomalous diffusion of ions in cells, and memory effects in epidemic spreading and microbial growth),^{23,28–34} to name a few.

The study of coupled fractional-order systems has attracted a lot of attention in the past few decades, in particular, as regards the synchronization of chaotic fractional-order systems.^{35–40} However, although much work has been done on symmetry-breaking phenomena, their investigation in coupled fractional-order systems is only in its debut. The impact of fractional derivatives on oscillation death was considered for the first time by some of us in Ref. 41, which triggered a wave of interesting works on the study of quenching phenomena (amplitude death and oscillation death) in coupled fractional-order systems.^{42–46} Overall, these studies yield similar conclusions, namely, that fractional derivatives have a stabilizing effect. On the other hand, the investigation of chimera states in fractional-order systems has only recently become a focus of research, the very first reports on this subject dating from 2020.^{47,48} Recently, we considered a network of fractional-order Stuart–Landau oscillators in this context,¹¹ and we found that fractional derivatives impact deeply the behavior of the network. As the order of fractional derivatives decreases, the lifetime of amplitude chimeras is extended up to a critical value of the derivatives order where there is a transition to a novel amplitude chimera that is transient to oscillation death. A further decrease in the order of fractional derivatives promotes diverse oscillation death and chimera death states and inhibits the in-phase synchronized state and amplitude chimeras, as a consequence of the aforementioned stabilizing effect of fractional derivatives.

In the present work, we proceed with the study of symmetry-breaking phenomena in coupled fractional-order systems by considering fractional-order counterparts of two other famous limit cycle oscillators, namely, the van der Pol and Rayleigh oscillators. Like the Stuart–Landau oscillator, the van der Pol oscillator is a paradigmatic model widely used for studying symmetry-breaking phenomena, namely, oscillation death^{15,45,49–53} and chimera states.^{14,54–57} In these previous works, the equations of the van der Pol oscillator were written in the classical form, i.e., a second-order differential equation with a nonlinear damping term, and it

was found that the corresponding coupled systems exhibit phase chimeras and amplitude mediated chimeras.^{14,54–57} In the present work, we consider the van der Pol oscillator in the Liénard plane,⁵⁸ obtained by applying the Liénard transformation to the classical van der Pol model.^{59,60} And, it is found for the first time that a network of this form of the van der Pol model exhibits amplitude chimeras. On the other hand, the Rayleigh oscillators has been less considered in the context of studies on symmetry-breaking phenomena. It was found that oscillation death and amplitude chimeras can emerge in a network of Rayleigh oscillators with direct couplings.¹⁶ In Ref. 61, it was shown that cross couplings can induce a transition from amplitude chimera to amplitude mediated chimeras and variable-amplitude chimeras in a network of Rayleigh oscillators.

By considering two other limit-cycle oscillator models (the van der Pol and Rayleigh oscillators), we intend to generalize the results of the work reported in Ref. 11 where symmetry-breaking states were studied in a network of fractional-order Stuart–Landau oscillators. For better comparison, the networks of the two models considered here are set in the same conditions as the network in Ref. 11, i.e., the same size, the same coupling scheme, and the same initial conditions. As regards the coupling scheme, each oscillator of these two networks is diffusively and directly coupled to all its counterparts, and the coupling strength decays in a power-law fashion with the lattice distance—a realistic coupling scheme that interpolates between the nearest-neighbor (local) and mean-field (global) limits, via nonlocal coupling.^{62,63} This coupling scheme has proved to favor the occurrence of oscillation death states and amplitude chimeras by tuning the coupling exponent.^{11,16,19} The initial conditions are specially prepared such that the networks can exhibit chimera states, including chimera death. Note that as networks of nonlocally coupled integer-order Stuart–Landau oscillators,^{11,13} the integer-order counterparts of the considered networks can exhibit amplitude chimeras and oscillation death states. As there is a similarity in the behavior of coupled systems of these three models, an interesting question arises naturally: what about the impact of fractional derivatives? The present work aims at solving the issues behind this question. The rest of the paper is structured as follows. In Sec. II, the networks models are described. Section III is devoted to the study of the basic dynamical features of the uncoupled units that are fractional-order van der Pol and Rayleigh oscillators, which reveals that each of them undergoes a supercritical Hopf-like bifurcation as the order of the derivatives decreases. The dynamical behavior of the two networks are explored numerically and analytically in Sec. IV. In this section, the integer-order counterparts of the two networks are studied first, which reveals that they can exhibit simple oscillation death patterns and two types of amplitude chimeras that are transient to synchronization and oscillation death, respectively. Then, the stability of asymptotic states are analyzed in order to predict the effect of fractional derivatives on the occurrence and on the characteristics of these states. At last, the dynamical behavior of the fractional-order oscillator networks are explored numerically, and the analytical stability results are confirmed. In particular, the effect of fractional derivatives on amplitude chimeras is discussed. The paper ends with a conclusion in Sec. V where the main results of this work are summarized.

II. NETWORK MODELS

We study two networks of fractional-order van der Pol and Rayleigh oscillators, respectively. Each network is made up of N identical fractional-order oscillators, where the coupling is global with a weighted coupling strength decreasing with distance according to a power-law.^{62,63} The coupling is diffusive and direct through one of the two dynamical variables. Let $\mathbf{x} = (x \ y)^T$ be the vector of dynamical variables of an uncoupled unit, $\mathbf{F}(\cdot)$ the vector function describing the local dynamics, \mathbf{G} the global power-law connectivity matrix, $\mathbf{H}(\cdot)$ the vector function specifying which one of the two variables is involved in the direct diffusive coupling between two units, and $\sigma \in \mathbb{R}_+$ the coupling strength. Then, each network of coupled fractional-order oscillators is described by the following generic set of fractional-order differential equations:

$$D_t^\alpha \mathbf{x}_k = \mathbf{F}(\mathbf{x}_k) + \frac{\sigma}{\eta} \sum_{j=1}^N G_{kj} \mathbf{H}(\mathbf{x}_j), \tag{1}$$

where $k = 1, 2, \dots, N$, and periodic boundary conditions are assumed; $G_{kk} = -\eta$, $G_{k,k-r} = G_{k,k+r} = 1/r^s$, for $r = 1, \dots, P-1$, and $G_{k,k-P} \equiv G_{k,k+P} = 1/P^s$, $\eta = 2 \sum_{r=1}^{P-1} (1/r^s) + 1/P^s$ is a normalization factor, with $P = N/2$ and N is even; and $s \in \mathbb{R}_+$ is the coupling exponent. In the term $D_t^\alpha \mathbf{x}$, $\mathbf{a} = (\alpha \ \alpha)^T$, and D_t^α is the fractional derivative operator that, applied to a given dynamical variable, denotes its derivative of order α with respect to time t , where $\alpha \in \mathbb{R}_+$. We use Caputo's definition of fractional derivative since with this it is not necessary to define the fractional-order initial conditions.²⁰ It is given by (see Ref. 64)

$$D_t^\alpha x(t) = \frac{1}{\Gamma(n-\alpha)} \int_0^t \frac{x^{(n)}(\tau)}{(t-\tau)^{\alpha-n+1}} d\tau, \tag{2}$$

where $n-1 < \alpha < n \in \mathbb{N}$ and $\Gamma(\cdot)$ is the Gamma function. Two types of local dynamics are considered, namely, the van der Pol oscillator (whose equations are written in the Liénard plane^{58–60}) for which

$$\mathbf{F}(\mathbf{x}) = \begin{pmatrix} (y + x - x^3/3)/\varepsilon \\ -x \end{pmatrix}, \tag{3}$$

and the Rayleigh oscillator⁶⁵ for which

$$\mathbf{F}(\mathbf{x}) = \begin{pmatrix} \omega y \\ \mu(1-y^2)y - \omega x \end{pmatrix}. \tag{4}$$

The vector function $\mathbf{H}(\mathbf{x}) = \mathbf{E}\mathbf{x}$, where $\mathbf{E} = \begin{pmatrix} 0 & 0 \\ 0 & 1 \end{pmatrix}$ for the network of van der Pol oscillators and $\mathbf{E} = \begin{pmatrix} 1 & 0 \\ 0 & 0 \end{pmatrix}$ for the network of Rayleigh oscillators. The coupling exponent s (along with the normalization factor η) allows us to interpolate between the nearest-neighbor ($s \rightarrow \infty, \eta \rightarrow 2$) and mean-field ($s = 0, \eta = N-1$) limit topologies. Thus, $\eta/(2N)$ can be conceived as the normalized coupling radius, i.e., the coupling range.

In the following, we give a brief derivation of the van der Pol model in the version of Eq. (3) from the classical van der Pol

equation:

$$\ddot{v} - \mu(1 - v^2)\dot{v} + v = 0, \tag{5}$$

where v is the dynamical variable, μ is the nonlinearity parameter, and the dot over v denotes the first-order derivative with respect to time. If one applies the Liénard transformation^{59,60}

$$y = -v + \frac{v^3}{3} + \frac{\dot{v}}{\mu}, \tag{6}$$

in Eq. (5), then it is transformed into the following first-order differential equation:

$$\mu\dot{y} = -v. \tag{7}$$

Associating Eqs. (6) and (7) and rescaling the time in these two equations by applying the transformation $t \rightarrow t/\mu$, one obtains the following set of first-order differential equations:

$$\begin{aligned} \dot{x} &= \frac{1}{\varepsilon} \left(y + x - \frac{x^3}{3} \right), \\ \dot{y} &= -x, \end{aligned} \tag{8}$$

where $x = v$ and $\varepsilon = 1/\mu^2$. By this equation, the van der Pol model is written in the Liénard plane (x, y) . Thus, one uncovers the version of the van der Pol model considered in this work [see Eq. (3)]. The FitzHugh–Nagumo model^{66,67} (also known as the Bonhoeffer–van der Pol model⁶⁶) is closely related to this form of the van der Pol equation.

We are all familiar with the integer-order version of Eq. (1), where the term on the left hand side is the first-order derivative of the vector \mathbf{x} . Indeed, much dynamical systems are described by sets of first-order differential equations. However, experimental evidence suggests that in some cases, the first-order derivatives should be replaced by real-number-order derivatives. For example, the voltage–current characteristics of a real capacitor is given by $i(t) = C_\alpha D_t^\alpha v(t)$, where C_α is a parameter related to the capacitance C of the capacitor and α is a positive real number lesser than 1 that is related to the dielectric losses in the capacitor.²⁴ The values of C_α and α depend on the kind of dielectrics and some of these coefficients can be found in Refs. 24 and 26 for real capacitors. For an ideal capacitor, $\alpha \rightarrow 1$ and $C_\alpha = C$. Another classical example is provided by the theory of viscoelasticity: For the description of viscoelastic materials, one should consider the existence of a third element known as the spring-pot whose properties are intermediate between the spring and the dashpot.²¹ The stress $\sigma(t)$ of a spring-pot is proportional to the fractional derivative of the strain $\varepsilon(t)$ (see Ref. 21): $\sigma(t) = E(F/E)^\alpha D_t^\alpha \varepsilon(t)$, where F is the coefficient of viscosity for the corresponding dashpot element and E is the modulus of elasticity for the corresponding spring element, and $0 < \alpha < 1$. The spring-pot interpolates between the spring ($\alpha \rightarrow 0$) and the dashpot ($\alpha \rightarrow 1$).

Taking into account the above arguments, we consider the network model given by Eq. (1) for $0 < \alpha < 1$, which is a generalization of the integer-order model, as $\lim_{\alpha \rightarrow 1} D_t^\alpha x = dx/dt$ (see Ref. 64).

Before investigating the coupled dynamics, it is necessary to discuss the basic behavior of a single fractional-order oscillator of each network.

III. THE UNCOUPLED FRACTIONAL-ORDER OSCILLATOR

In case the N oscillators of a considered network are uncoupled, i.e., for $\sigma = 0$ in Eq. (1), this set of equations degenerates into those of one oscillator, i.e.,

$$D_t^\alpha \mathbf{x} = \mathbf{F}(\mathbf{x}), \tag{9}$$

where $\mathbf{F}(\mathbf{x})$ is given either by Eq. (3) or by Eq. (4). The parameters ε , ω , and μ are chosen such that the dynamics of the integer-order counterparts of the two considered oscillators are characterized by self-sustained oscillations around the unique equilibrium point $E(x_E = 0, y_E = 0)$ whose stability changes via a Hopf bifurcation when a parameter varies. The fractional derivative affects neither the number of equilibrium points of a system nor their positions, but it may change their stability. So, it is appropriate to study the stability of E in this particular context. Let $\{\lambda\}$ be the eigenvalues spectrum of the Jacobian matrix of the uncoupled system evaluated at E . According to the stability theorem of commensurate fractional-order systems,²⁰ the equilibrium point E is asymptotically stable if all the eigenvalues $\lambda_{1,2}$ satisfy the condition $|\arg(\lambda_{1,2})| > \alpha\pi/2$, which can be rewritten as $|\text{Im}(\lambda_{1,2})/\text{Re}(\lambda_{1,2})| > \tan(\alpha\pi/2)$. For the van der Pol oscillator, $\lambda_{1,2} = (1 \pm i\sqrt{4\varepsilon - 1})/(2\varepsilon)$ (where $i^2 = -1$ and $\varepsilon > 1/4$), and the stability condition is

$$\alpha < \frac{2}{\pi} \tan^{-1} \sqrt{4\varepsilon - 1}. \tag{10}$$

For the Rayleigh oscillator, $\lambda_{1,2} = (\mu \pm i\sqrt{4\omega^2 - \mu^2})/2$ (where $\mu < 2\omega$), and the stability condition is

$$\alpha < \frac{2}{\pi} \tan^{-1} \frac{\sqrt{4\omega^2 - \mu^2}}{\mu}. \tag{11}$$

It was proved in Ref. 68 that periodic solutions do not exist in fractional-order autonomous systems involving fractional-order derivatives with bounded lower limit of the integral. However, such a system may have S -asymptotically T -periodic functions as solutions, instead of T -periodic solutions.⁶⁹ Thus, for the fractional-order oscillators considered, we assume that the nonlinearities are rather weak so that the solution of an uncoupled oscillator is an S -asymptotically T -periodic function if the equilibrium E is unstable, which retains the classical form $x(t) = A \cos(\Omega t)$, and the corresponding expression for $y(t)$. Note that $y(t)$ is also a sinusoidal function of time whose frequency is equal to Ω and amplitude depends on A and eventually on some parameters of the system. According to Eq. (2), $D_t^\alpha x(t) = A D_t^\alpha \cos(\Omega t)$. Since we are looking for asymptotic solutions, we need to utilize the asymptotic expression of Caputo's fractional derivative of the cosine function, i.e., $\lim_{t \rightarrow \infty} D_t^\alpha \cos(\Omega t) = \Omega^\alpha \cos(\Omega t + \alpha\pi/2)$ (see Ref. 70). Introducing these expressions into Eq. (9) [associated with Eqs. (3) and (4)], we find that the amplitude A and the frequency Ω are given by

$$A = 2\sqrt{1 - 2\sqrt{\varepsilon} \cos \frac{\alpha\pi}{2}} \quad \text{and} \quad \Omega = \varepsilon^{-\frac{1}{2\alpha}} \tag{12}$$

for the van der Pol oscillator, and

$$A = \frac{2}{\sqrt{3}} \sqrt{1 - \frac{2\omega}{\mu} \cos \frac{\alpha\pi}{2}} \quad \text{and} \quad \Omega = \omega^{\frac{1}{\alpha}} \quad (13)$$

for the Rayleigh oscillator.

These oscillatory solutions do not exist when $A^2 < 0$; then, the oscillations are quenched, which means that the equilibrium point E of each fractional-order oscillator loses stability via a Hopf-like bifurcation when $A^2 = 0$. Actually, in a strict sense, Hopf bifurcation cannot occur in a fractional-order system as here an exact periodic solutions on a finite time interval is not possible.⁶⁸ Therefore, the concept of Hopf-like bifurcation was introduced in Ref. 71 to characterize the change of stability of an equilibrium point giving rise to the birth of S -asymptotically T -periodic solutions. Applying the condition $A^2 = 0$ in Eqs. (12) and (13), we obtain that a Hopf-like bifurcation occurs at $\alpha = \alpha_H$, where $\alpha_H = 2 \tan^{-1}(\sqrt{4\varepsilon - 1})/\pi$ for the fractional-order van der Pol oscillator and $\alpha_H = 2 \tan^{-1}(\sqrt{4\omega^2 - \mu^2}/\mu)/\pi$ for the fractional-order Rayleigh oscillator. These results are in perfect agreement with the results of local stability analysis given by Eqs. (10) and (11). Figure 1 shows an illustration of these results, where the numerical results are obtained by solving the set of fractional differential equations (9) [associated with Eqs. (3) and (4)] with the Adams–Bashforth–Moulton predictor–corrector scheme^{72,73}—developed on the basis of Caputo’s definition of fractional derivative [given by Eq. (2)]. Figure 1 shows that as the order of fractional derivatives decreases, the amplitude of oscillations decreases up to $\alpha = \alpha_H$ where a supercritical Hopf-like bifurcation occurs. This means that oscillatory behaviors should be expected in the network only for $\alpha > \alpha_H$. In the following, the network behavior is explored for α values within this range. As regards the variations of A with respect to α , we see that there is a striking similarity between the subsets (a) and (b) of Fig. 1. We should also point out the striking similarity with the behavior of the radius of the limit cycle of the fractional-order Stuart–Landau oscillator.^{11,41}

IV. THE NETWORK DYNAMICS

Here, we investigate two networks of $N = 100$ identical fractional-order van der Pol and Rayleigh oscillators, respectively, described by Eq. (1) associated with Eqs. (3) and (4). Throughout the paper, the coupled systems are studied for parameters used in Fig. 1. As control parameters, we consider the coupling parameters σ and s , and the derivatives order α . For the numerical solution of the coupled system, we employ initial conditions as in Ref. 11: $(x_k(0), y_k(0)) = (0, -1)$ for $k \in [1, N/4] \cup (3N/4, N] \equiv (-N/4, N/4] = (-25, 25]$ and $(x_k(0), y_k(0)) = (0, rand_k)$ for $k \in (N/4, 3N/4) = (25, 75]$, where $rand_k$ are elements of a random sequence of real numbers in $[0, 1]$.

A. Dynamical behavior of the networks of integer-order oscillators

The sets of differential equations describing the networks of integer-order elements [Eq. (1) for $\alpha \rightarrow 1$, along with Eqs. (3)

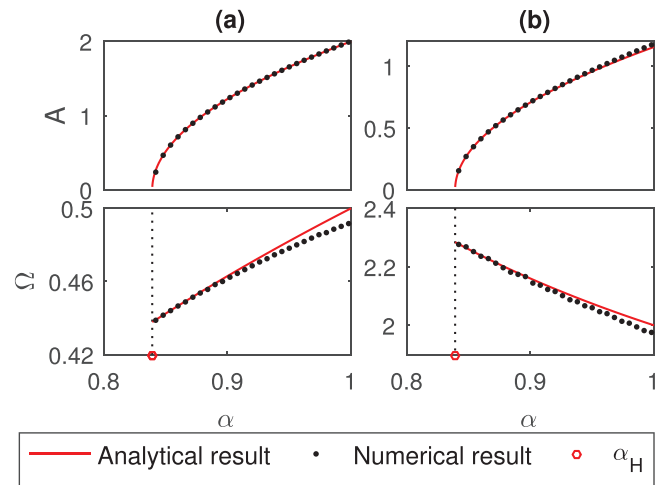


FIG. 1. Amplitude and frequency of the periodic solution $x(t) = A \cos(\Omega t)$ of the fractional-order oscillators vs fractional derivatives order α : (a) van der Pol oscillator for $\varepsilon = 4$ and (b) Rayleigh oscillator for $\omega = 2$ and $\mu = 1$. At these parameter values, $\alpha_H \approx 0.839$ for the two fractional-order systems.

and (4)] are solved numerically thanks to the fourth-order Runge–Kutta method.

Depending on the parameter values, the network of van der Pol oscillators may exhibit three prominent asymptotical dynamical states shown in Fig. 2: a two-cluster coherent OD state that we will call coherent OD [see Fig. 2(a)], the in-phase synchronized state in Fig. 2(b), and another OD state that we will call alternating OD [see Fig. 2(c)]. The in-phase synchronization and alternating OD regimes are eventually preceded by chimera states as shown in Figs. 2(b) and 2(c).

In the case of coherent OD, obtained for small values of s (including $s = 0$: global coupling), the network is split up in two subpopulations with identical sizes: one population of oscillators lying on the upper steady state branch, where $x_k(t) \approx +x_*$ for $k \in (N/4, 3N/4) = (25, 75]$ (corresponding to the incoherent region of the initial state), and the other population of oscillators lying on the lower steady state branch $x_k(t) \approx -x_*$, where x_* is a positive constant number. In the case of alternating OD states, obtained for higher values of s , adjacent oscillators populate alternately one of the two branches ($-x_*$ and $+x_*$) of the inhomogeneous steady state, almost all through the network [see the snapshot in Fig. 2(c)]. However, the degree of coherence decreases with increasing value of the coupling strength σ . The incoherence appears here in two ways: on the one hand, two adjacent oscillators may populate the same branch of the OD, and on the other hand, even if adjacent oscillators populate alternating branches of the OD, equivalent levels (either upper or lower branch) may not exactly coincide.

The network of Rayleigh oscillators behaves almost in the same way. Besides the prominent dynamical regimes obtained in the case of the network of van der Pol oscillators, there are two other types of OD states that appear in narrow regions of the parameter s at the transition from coherent OD state to in-phase synchronized state,

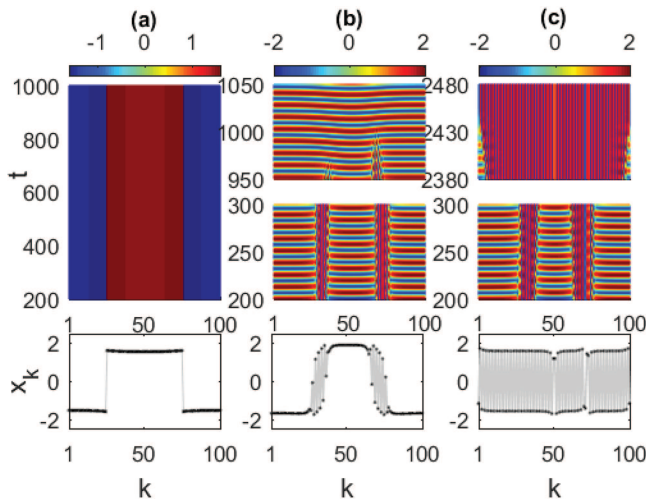


FIG. 2. Space–time plots $x_k(t)$ and snapshots $x_k(t_{\text{Snap}})$ of the collective dynamical states exhibited by the network of integer-order van der Pol oscillators for $\varepsilon = 4$ as in Fig. 1, and different values of s and σ : (a) $s = 0.35$ and $\sigma = 5.6$: coherent OD (COD); (b) and (c) $s = 3.5$ and (b) $\sigma = 2.5$: chimera state transient to the in-phase synchronized state (Sync); and (c) $\sigma = 3.5$: chimera state transient to alternating OD (AOD). Snapshots at $t_{\text{Snap}} = 300$ for (a) and (b) and at $t_{\text{Snap}} = 2480$ for (c).

namely, solitary OD states. In a solitary OD state [see Figs. 3(b) and 3(c)], some solitary oscillators break away from the upper branch of the coherent OD state. So, one obtains solitary steady states within the coherent OD pattern.¹¹ The solitary steady states that appear only in the incoherent region of the initial state, i.e., for $k \in (N/4, 3N/4) = (25, 75)$, are randomly distributed in this region. By m -cluster solitary OD, we denote an OD pattern with an incoherent region involving solitary steady states and a coherent region that is split up in m clusters. The number of solitary steady states in a solitary OD pattern increases with increasing value of the coupling exponent s .

In what follows, we will determine the type of chimera states observed in the two networks using some quantitative measures.

B. Dynamical regimes characterization using quantitative measures

In order to check whether the chimera states mentioned above (see Figs. 2 and 3) are pure amplitude chimeras or amplitude mediated chimeras, we use the mean phase velocity profile $\{\omega_k = 2\pi M_k / \Delta t, k = 1, 2, \dots, N\}$, where M_k is the number of periods or pseudo-periods performed by the k th unit in the time interval Δt (see Refs. 61 and 74). A period or pseudo-period is the elapsed time between two consecutive maxima of a dynamical variable. The term pseudo-period is used in the case of the amplitude chimeras that are asymptotically transformed to alternating OD where the oscillators belonging to incoherent regions do not show periodic oscillations because of the drifting and damping phenomena characterizing their dynamics.¹¹ Indeed, the mean phase velocity profile is typically arc-shaped for incoherence with respect to the

phase, while it is flat for coherence of phases. We plotted the mean phase velocity profile for the chimera states shown in Figs. 2(b), 2(c), 3(d), and 3(e) and found that all these profiles are flat, showing the total coherence of phases in all these chimera states. In consequence, the chimera states obtained in this work are pure amplitude chimeras, known as amplitude chimeras.

To further characterize the amplitude chimeras obtained in this work, we use some pertaining quantitative measures developed in Ref. 13. The center of mass (c.m.) of the oscillator on the site k is given by

$$x_k^{c.m.}(t) = \frac{1}{T} \int_t^{t+T} x_k(\tau) d\tau, \tag{14}$$

where $T = 2\pi / \Omega$, with Ω defined in Eqs. (12) and (13). A similar definition holds for $y_k^{c.m.}(t)$. For the k th oscillator, the shift of the center of mass from the origin is given by

$$z_k^{c.m.}(t) = \sqrt{[x_k^{c.m.}(t)]^2 + [y_k^{c.m.}(t)]^2}. \tag{15}$$

The quantities $x_k^{c.m.}$, $y_k^{c.m.}$, and $z_k^{c.m.}$ can serve as local order parameters, as they vanish for the nodes within the coherent regions of an amplitude chimera, whereas all the nodes within the incoherent regions have non-zero finite values, allowing to distinguish between coherent and incoherent regions.

The degree of incoherence of an amplitude chimera can be measured by the relative size of the incoherent regions that can serve as a global order parameter derived from the above local order parameter $z_k^{c.m.}(t)$. The size of incoherent regions (S_{Inc}) is the relative number of drifting oscillators given by the total number of drifting oscillators (N_{Drift}) normalized by the overall number of oscillators within the whole network as follows:

$$S_{\text{Inc}}(t) = \frac{N_{\text{Drift}}(t)}{N} = \frac{1}{N} \sum_{k=1}^N H(z_k^{c.m.}(t) - \delta), \tag{16}$$

where $H(\cdot)$ is the Heaviside function and δ is a predefined small threshold number chosen such as $z_k^{c.m.}(t) < \delta$ when the node k belongs to a coherent region of the amplitude chimera state.

A long-living or stable amplitude chimera is characterized in the course of time by non-drifting and constant size incoherent regions, constant amplitudes, and fixed shifts of center of mass of drifting units' oscillations (see Fig. 4). However, we obtain here another type of amplitude chimera [as shown in Figs. 2(c) and 3(e)] whose incoherent region(s) size grows in the course of time (see the time evolution of S_{Inc} in Fig. 5) and drifting units are characterized by damped oscillations as shown in Fig. 5. An oscillator k belongs to the coherent region when $x_k^{c.m.}(t) = 0$, then it starts drifting when the value of $x_k^{c.m.}(t)$ starts drifting from the zero value—this situation is illustrated in Fig. 5 for the unit $k = 20$. This oscillator starts drifting at $t \approx 840$ and afterward, the oscillations are continuously damped until they are quenched at $t \approx 2440$. This is the case for all the oscillators; only the beginning instant of the drifting changes from one oscillator to another. We make the same observations in the behavior of the network of Rayleigh oscillators. Thereafter, the amplitude chimera transient to synchronization will be referred to as classical amplitude chimera and the amplitude chimera transient to OD will be referred to as damped amplitude chimera. The damped

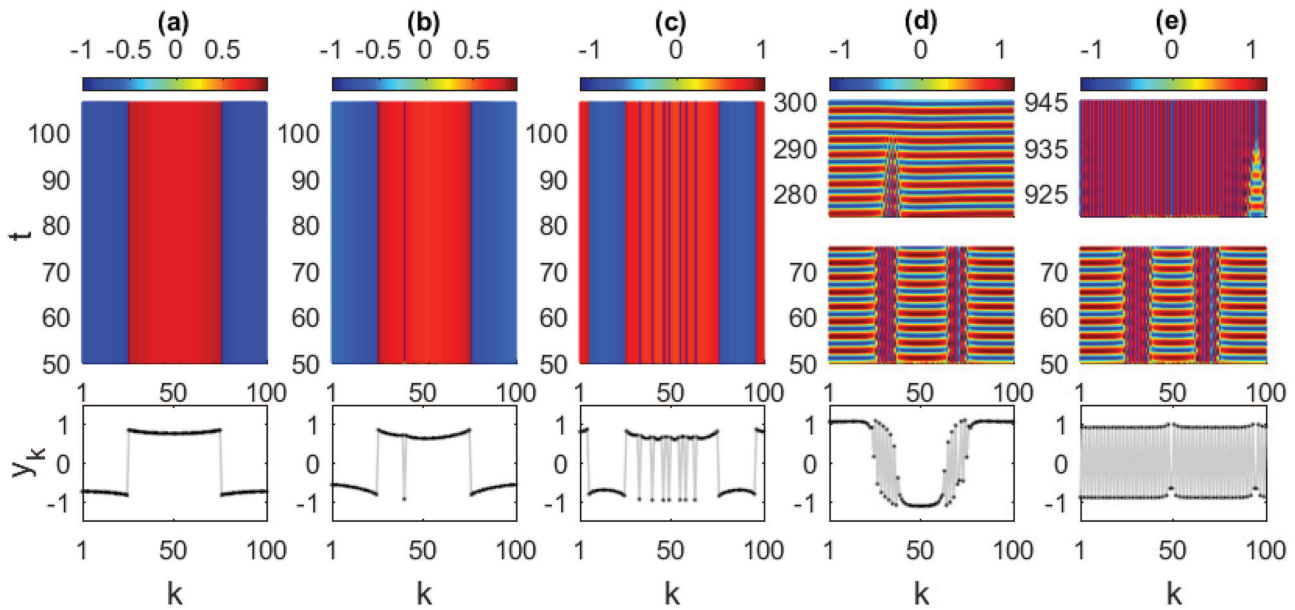


FIG. 3. Space–time plots $y_k(t)$ and snapshots $y_k(t_{\text{Snap}})$ of the collective dynamical states exhibited by the network of integer-order Rayleigh oscillators for $\omega = 2$ and $\mu = 1$ as in Fig. 1, and different values of s and σ : (a)–(c) $\sigma = 14$ and (a) $s = 0.5$: coherent OD (COD); (b) $s = 0.78$: one-cluster solitary OD (1-SOD); (c) $s = 0.95$: three-cluster solitary OD (3-SOD); (d) and (e) $s = 3.5$ and (d) $\sigma = 11.2$: chimera state transient to the in-phase synchronized state (Sync); and (e) $\sigma = 13.2$: chimera state transient to alternating OD (AOD). Snapshots at $t_{\text{Snap}} = 75$ for (a)–(d) and at $t_{\text{Snap}} = 945$ for (e).

amplitude chimera was observed for the first time in a network of Rayleigh oscillators,¹⁶ and subsequently, its occurrence was shown to be induced by fractional derivatives in a network of Stuart–Landau oscillators.¹¹

As a global order parameter, $S_{\text{Inc}}(t)$ is used to identify the prominent dynamical states that the networks exhibit and to detect the transitions between these states. Indeed, as shown in Fig. 6, $S_{\text{Inc}}(t) = 0 \forall t$ for the in-phase synchronized state, $S_{\text{Inc}}(t) = 1 \forall t$ for alternating OD states, and $0 < S_{\text{Inc}}(t) < 1$ for amplitude chimeras.

In order to provide an overall view on the network behavior for a wide range of coupling parameters, the dynamical regimes maps in

the plane of coupling exponent (s) and coupling strength (σ) is produced (see Fig. 7) with the help of the global order parameter S_{Inc} . As S_{Inc} is no longer of any use in making the distinction between the different OD states, we use the intrinsic properties of these patterns,

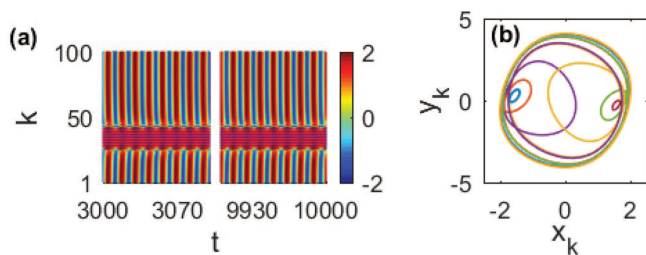


FIG. 4. Long-living amplitude chimera occurring in the network of integer-order van der Pol oscillators for $\varepsilon = 4$ as in Fig. 1, $s = 3.5$, and $\sigma = 3.02704$: (a) space–time plot for the variable x and (b) phase portraits $[x_k(t), y_k(t)]$ of selected oscillators, with $k \bmod 3 = 0$, and for $4000 < t < 8000$.

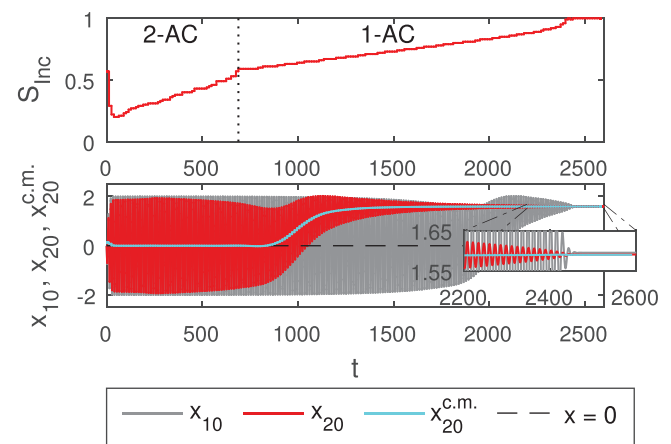


FIG. 5. Time series of the global order parameter S_{Inc} and time series $x_k(t)$ for two selected oscillators of the amplitude chimera pattern of Fig. 2(c). The two incoherent regions of the initial amplitude chimera collide at a certain time and the two-headed amplitude chimera (2-AC) is transformed into one-headed amplitude chimera (1-AC), which justifies the change of slope in the time series of S_{Inc} .

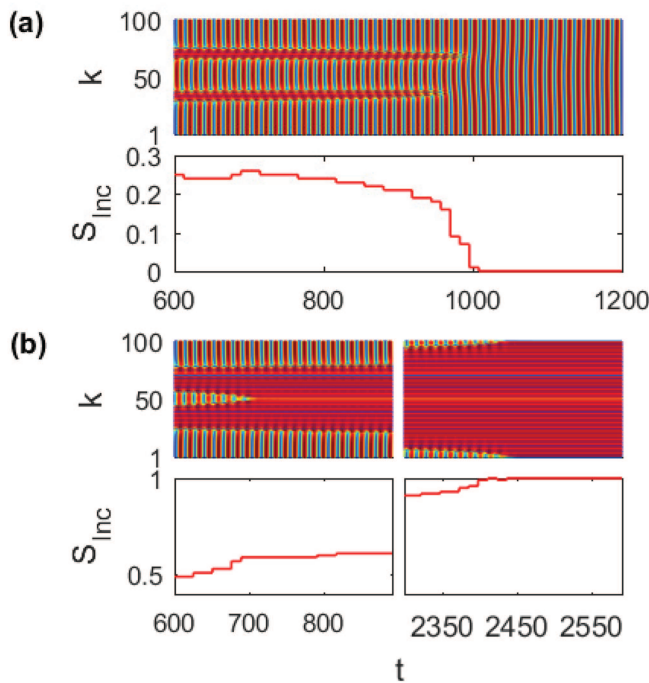


FIG. 6. Some collective dynamical regimes for integer-order van der Pol oscillators network with the corresponding time series of the global order parameter S_{Inc} : (a) dynamical regimes of Fig. 2(b): classical amplitude chimera and in-phase synchronization and (b) dynamical regimes of Fig. 2(c): damped amplitude chimera and alternating OD.

i.e., the way the oscillators are organized in these patterns. We see that there is a striking similarity between the two subsets (a) and (c) of Fig. 7 showing the mapping of the dynamical states occurring in networks of van der Pol oscillators and Rayleigh oscillators, respectively. A comparison with the results in Ref. 11 shows that there is also a similarity with the map, in the same parameter space, of the dynamical states occurring in a network of the same number of Stuart–Landau oscillators coupled in the same way and subject to the same initial conditions as in the present work.

Figures 7(b) and 7(d) show that there is a region in the parameter space where the transient amplitude chimeras are more and more important with high lifetimes (t_{Trans}) able to reach $4000T$, where T is the period of oscillation of an uncoupled unit. This region of amplitude chimeras with high lifetimes occurs at the transition from asymptotic in-phase synchronization to asymptotic alternating OD as the coupling strength σ varies for a fixed coupling exponent s . As the value of σ comes closer to the bifurcation point σ_C , the lifetime (t_{Trans}) of amplitude chimeras increases at the two sides, as shown in Fig. 8. However, the growth of the lifetime of classical amplitude chimeras is modest compared to the growth of the lifetime of damped amplitude chimeras. This is the reason why one should pay attention to the damped amplitude chimera. Figure 8 also shows that the growth of t_{Trans} follows the logarithmic law $t_{Trans}(\sigma) = b \log(|\sigma - \sigma_C|) + d$ in an exponentially narrow interval of the

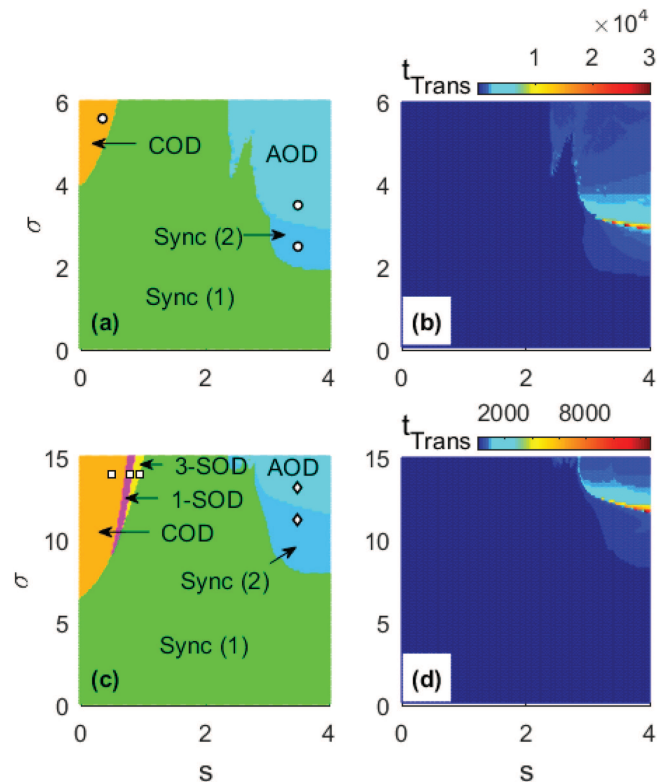


FIG. 7. Asymptotic dynamical regimes [(a) and (c)] and lifetime of transient regimes t_{Trans} [(b) and (d)] in the plane (s, σ) of coupling parameters. (a) and (b) Network of integer-order van der Pol oscillators for $\varepsilon = 4$ as in Fig. 1; (c) and (d) network of integer-order Rayleigh oscillators for $\omega = 2$ and $\mu = 1$ as in Fig. 1. Sync: in-phase synchronization, COD: coherent OD, AOD: alternating OD, 1-SOD: one-cluster solitary OD, and 3-SOD: three-cluster solitary OD. The asymptotic alternating OD regime is preceded by an amplitude chimera with noticeable lifetime, whereas the asymptotic in-phase synchronized state regime is sometime preceded by an amplitude chimera. For the sake of visibility, the asymptotic in-phase synchronized state region is split up in two subdomains according to the range of the lifetime of transient amplitude chimera states: $t_{Trans} < 50T$ in the region labeled Sync (1), and $t_{Trans} \geq 50T$ in the region labeled Sync (2), where T is the period of oscillation of an uncoupled unit. The circle, square, and diamond markers show the parameter values used for Figs. 2, 3(a)–3(c), and 3(d) and 3(e), respectively. Note that extending the range of σ in (a) up to 15 as in (c) does not bring any important information since no new state appears.

bifurcation parameter σ . Similar behavior of the lifetime of the classical amplitude chimera with respect to the coupling parameters was observed in networks of Stuart–Landau oscillators⁷⁵ and Rayleigh oscillators¹⁶ under phase–antiphase (or antisymmetric) distribution of initial conditions. Indeed, under such initial conditions, these networks exhibit long-living, even stable classical amplitude chimeras in the parameter space at the interface between the asymptotic in-phase synchronized state and asymptotic OD states.

Furthermore, it is interesting to investigate how the network size influences the dynamical regimes attained by the two networks. To do so, we increase the size of each network from $N = 100$ oscillators

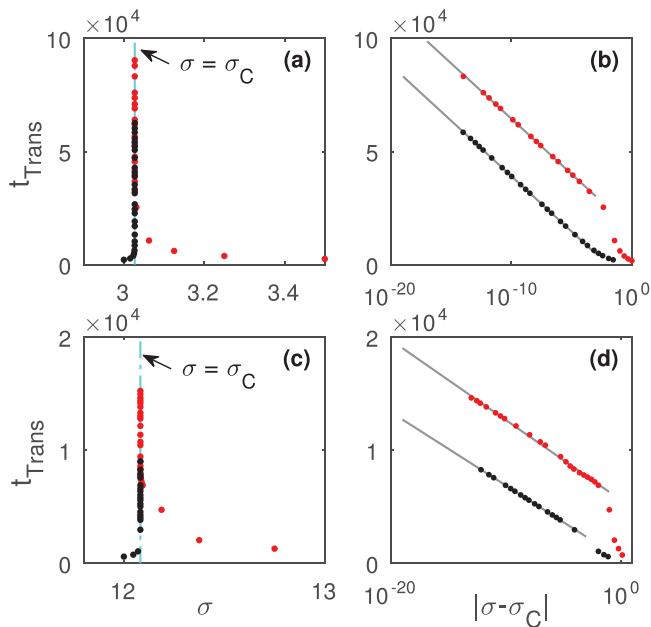


FIG. 8. Amplitude chimeras lifetime t_{Trans} vs coupling strength σ and vs the shift $|\sigma - \sigma_C|$ in the logarithmic scale, where σ_C marks the threshold between classical amplitude chimeras and damped amplitude chimeras. Black (respectively, red) dots for classical (respectively, damped) amplitude chimeras. Network of integer-order van der Pol oscillators (a) and (b); network of integer-order Rayleigh oscillators (c) and (d). The gray lines in (b) and (d) are fitting curves with the formula $t_{\text{Trans}}(\sigma) = b \log(|\sigma - \sigma_C|) + d$, where b and d are different sets of fit parameters for each curve. For this figure, $s = 3.5$, and other parameters as in Fig. 1.

to $N = 200$. Keeping the same initial conditions as above, the two networks are studied using numerical simulations. For the two networks, we observe the same dynamical states as above. However, the region of existence of asymptotic alternating OD states in the plane (s, σ) shifts significantly to higher values of the coupling strength σ in the case of the network of van der Pol oscillators. In other words, the transition from the in-phase synchronized state to alternating OD states occurs at higher values of σ compared to the case $N = 100$. As a consequence, the growth of the lifetime of amplitude chimeras observed for $N = 100$ as the value of σ approaches the transition point σ_C is not anymore observed. Overall, in the case of the network of van der Pol oscillators, the lifetime of classical amplitude chimeras decreases with increasing size of the network, a phenomenon observed in networks of Stuart–Landau oscillators.⁷⁶ Contrarily, in the case of the network of Rayleigh oscillators, the position of the transition point σ_C does not vary significantly. So, the growth of the lifetime of the chimera states is still observed as confirmed by Fig. 9. In addition, as shown by this figure, the rate of growth of the chimeras lifetime increases with increasing size of the network. Interestingly, as the value of the coupling strength σ decreases coming closer to σ_C , damped amplitude chimera states disappear at $\sigma = \sigma_S$ and the amplitude chimeras become stable. In

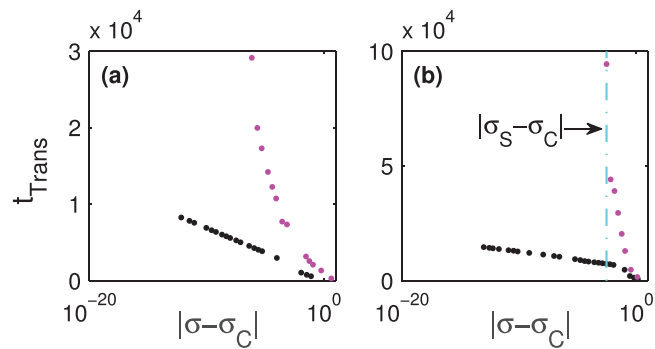


FIG. 9. Lifetime t_{Trans} of amplitude chimeras occurring in networks of integer-order Rayleigh oscillators vs $|\sigma - \sigma_C|$ in the logarithmic scale, where σ_C marks the threshold between classical amplitude chimeras and damped amplitude chimeras: (a) classical amplitude chimeras and (b) damped amplitude chimeras. Black (respectively, magenta) dots for $N = 100$ (or $N = 200$, respectively). For this figure, $s = 3.5$, and other parameters as in Fig. 1(b). σ_S is the critical value of σ at which there is transition from damped amplitude chimeras to stable amplitude chimeras.

this case, the bifurcation scenario can be read as follows: classical amplitude chimeras for $\sigma < \sigma_C$, stable amplitude chimeras for $\sigma_C < \sigma < \sigma_S$, and damped amplitude chimeras for $\sigma > \sigma_S$. We believe that the growth of the lifetime of chimera states might become more and more drastic as the size of the network increases, and as a consequence, the region $\sigma_C < \sigma < \sigma_S$ of stable amplitude chimeras might get larger.

The results depicted in Fig. 7 rely on the extensive numerical simulations. In Sec. IV C, we will perform the stability analysis of the in-phase synchronized state, coherent OD and alternating OD states in order to verify the results of numerical simulations and to predict the effect of fractional derivatives.

C. Linear stability analysis of dynamical states

For the study of the stability of the in-phase synchronized state, coherent OD, and alternating OD states, we make use of the properties of the variational equations of the coupled fractional-order systems. Let us recall that for certain parameter values, the in-phase synchronized state and alternating OD states are asymptotic states preceded by amplitude chimeras. The linear stability analysis proceeds in the same way as for the Stuart–Landau fractional-order oscillator.¹¹

We investigate the stability of a given state \mathbf{x}_* by considering small perturbations $\delta \mathbf{x}_k = \mathbf{x}_k - \mathbf{x}_*$. By linearizing Eq. (1) around \mathbf{x}_* we obtain the following variational equations:

$$D_t^\alpha \delta \mathbf{x}_k = DF(\mathbf{x}_*) \delta \mathbf{x}_k + \frac{\sigma}{\eta} \sum_{j=1}^N G_{kj} \mathbf{E} \delta \mathbf{x}_j, \quad (17)$$

where $k = 1, 2, \dots, N$ and $DF(\mathbf{x}_*)$ is the Jacobian matrix of the vector function $\mathbf{F}(\cdot)$ evaluated on \mathbf{x}_* . Equation (17) can be treated using the discrete Fourier transforms of the sequence

$\{\delta \mathbf{x}_k, k = 1, 2, \dots, N\}$ given by

$$\zeta_n = \frac{1}{\sqrt{N}} \sum_{j=1}^N \delta \mathbf{x}_j \exp\left(\frac{2\pi i j n}{N}\right), \quad (18)$$

where $n = 0, 1, 2, \dots, N - 1$ and $i^2 = -1$. Using the convolution theorem for discrete Fourier transforms,⁷⁷ Eq. (17) is block-diagonalized and it reduces to the following N independent variational equations:

$$D_t^\alpha \zeta_n = \left[DF(\mathbf{x}_*) + \frac{\sigma}{\eta} \gamma_n \mathbf{E} \right] \zeta_n, \quad (19)$$

where the eigenvalues of the connectivity matrix \mathbf{G} are given by

$$\gamma_n = -\eta + 2 \sum_{r=1}^{p-1} \left[\frac{1}{r^s} \cos\left(\frac{2\pi r n}{N}\right) \right] + \frac{(-1)^n}{P^s}. \quad (20)$$

Note that these N variational equations only differ by the dependence of γ_n on n , and that the sequence $\{\gamma_n, n = 1, 2, \dots, N - 1\}$ is symmetric with respect to $n = N/2$. Therefore, the study of N equations given by Eq. (17) is reduced to the study of $N/2 + 1$ equations given Eq. (19) for $n = 0, 1, 2, \dots, N/2$.

1. Linear stability of the in-phase synchronized state

The synchronous state \mathbf{x}_{Sync} defines the synchronization manifold $\{\mathbf{x}_k(t) = \mathbf{x}_{\text{Sync}}, \forall k = 1, 2, \dots, N\}$. Accordingly, in the case of synchrony of all oscillators, the coupling term in Eq. (1) vanishes and Eq. (1) reduces to the equation of an uncoupled oscillator. Thus, the state $\mathbf{x}_* = \mathbf{x}_{\text{Sync}}$ is the solution of Eq. (9). The in-phase synchronized state is characterized by the eigenmode $n = 0$ since $\gamma_0 = 0$, corresponding to the variational equation of an uncoupled oscillator. The study of the stability of the in-phase synchronized state is, thus, reduced to the study of the dynamical properties of the transverse eigenmodes [ruled by Eq. (19) for $n \neq 0$] which may be expressed by the conditional Lyapunov exponents $\lambda_n^{1,2} = \lim_{t \rightarrow +\infty} \ln(|\zeta_n^{1,2}|)/t$, where $n = 1, 2, \dots, N/2$ and $\zeta_n^{1,2}$ are the two components of ζ_n . A necessary condition for the linear stability of the in-phase synchronized state is that the maximum Lyapunov exponent must be negative,⁷⁸ i.e.,

$$\Lambda_{\text{Sync}} = \max_{n=1,2,\dots,N/2} (\max(\lambda_n^{1,2})) < 0. \quad (21)$$

Generally, the maximum Lyapunov exponent Λ_{Sync} as a function of the eigenvalues of \mathbf{G} is called master stability function, and it describes the stability of the network⁷⁸ when it is applied to all eigenvalues. Therefore, the behavior of the master stability function $\Lambda_{\text{Sync}}(\sigma, s, \alpha)$ in dependence on the parameters σ, s , and α will be considered in the following.

2. Stability of oscillation death states

An OD state is an inhomogeneous steady state where certain oscillators populate the branch $(x(t), y(t)) \approx (x_*, y_*)$ and the others populate the branch $(x(t), y(t)) \approx (-x_*, -y_*)$, where x_* and y_* are independent of time.

As mentioned above, the coherent OD state is defined as follows: $(x_k(t), y_k(t)) \approx (x_*, y_*)$ for $k \in (N/4, 3N/4]$ and

$(x_k(t), y_k(t)) \approx (-x_*, -y_*)$ elsewhere, and alternating OD states are defined as follows: $(x_k(t), y_k(t)) \approx (x_*, y_*)$ for k odd (or even, respectively) and $(x_k(t), y_k(t)) \approx (-x_*, -y_*)$ for k even (or odd, respectively). With this, the equations for the oscillator $k = 1$ can be derived from Eq. (1),

$$\begin{aligned} y_* + x_* - \frac{x_*^3}{3} &= 0, \\ -x_* - 2\sigma' y_* &= 0 \end{aligned} \quad (22)$$

for the network of van der Pol oscillators and

$$\begin{aligned} \omega y_* - 2\sigma' x_* &= 0, \\ \mu(1 - y_*^2) y_* - \omega x_* &= 0 \end{aligned} \quad (23)$$

for the network of Rayleigh oscillators, where $\sigma' = \sigma \left[1/(N/4)^s + 2 \sum_{r=N/4+1}^{p-1} (1/r^s) + 1/P^s \right] / \eta$ for the coherent OD state and $\sigma' = 2\sigma \sum_{r=0}^{N/4-1} [1/(2r+1)^s] / \eta$ for alternating OD states. Equations (22) and (23) admit a trivial solution, that is, $(x_*, y_*) = (0, 0)$, and eventually two other solutions that emerge due to the coupling, namely, $(x_*, y_*) = (x_-, y_-)$ and $(x_*, y_*) = (x_+, y_+)$,

$$x_{\pm} = \pm \sqrt{3 \left(1 - \frac{1}{2\sigma'} \right)}, \quad y_{\pm} = -\frac{x_{\pm}}{2\sigma'}, \quad (24)$$

for the network of van der Pol oscillators, with $\sigma' > \sigma'_p = 1/2$ and

$$x_{\pm} = \frac{\omega y_{\pm}}{2\sigma'}, \quad y_{\pm} = \pm \sqrt{1 - \frac{\omega^2}{2\mu\sigma'}}, \quad (25)$$

for the network of Rayleigh oscillators, with $\sigma' > \sigma'_p = \omega^2 / (2\mu)$. When the value of σ increases from 0, the trivial solution $(x_*, y_*) = (0, 0)$ is the only solution of Eqs. (22) and (23) until at $\sigma = \sigma_p$ (corresponding to σ'_p), a pitchfork bifurcation gives rise to the birth of two symmetric solutions (x_-, y_-) and (x_+, y_+) , which represent the emerging symmetry-breaking death states in the two networks.

The stability of these death states can be determined by the variational equations given by Eq. (19) with $\mathbf{x}_* = \mathbf{x}_+ = (x_+ \ y_+)^T$ and $\mathbf{x}_* = \mathbf{x}_- = (x_- \ y_-)^T$ and with the degenerate eigenvalues spectrum of Eq. (20). We substitute $\zeta_n \sim \exp(\lambda_{n\pm} t)$ into Eq. (19) and use $D_t^\alpha \zeta_n \sim \lambda_{n\pm}^\alpha \exp(\lambda_{n\pm} t)$ (see Ref. 70), where λ_{n+} and λ_{n-} are the eigenvalues associated with \mathbf{x}_+ and \mathbf{x}_- , respectively. Hence, $\lambda_{n\pm}$ are solutions of the characteristic equation,

$$\det \left(DF(\mathbf{x}_{\pm}) + \frac{\sigma}{\eta} \gamma_n \mathbf{E} - \lambda_{n\pm}^\alpha \mathbf{I}_2 \right) = 0, \quad (26)$$

where \mathbf{I}_2 is the 2×2 unit matrix. This equation can be rewritten as follows in the form of an algebraic equation:

$$\lambda_{n\pm}^{2\alpha} + b\lambda_{n\pm}^\alpha + c = 0. \quad (27)$$

Because, Eq. (27) contains only quadratic terms in x_{\pm} and y_{\pm} , and according to Eqs. (24) and (25), $x_-^2 = x_+^2$ and $y_-^2 = y_+^2$, we find

$\lambda_{n+} = \lambda_{n-}$. Thus, the two solutions $\lambda_{n+}^{1,2}$ of Eq. (27) are

$$\lambda_{n+}^{1,2} = \left(\frac{-b \pm \sqrt{\Delta}}{2} \right)^{\frac{1}{\alpha}}, \text{ or } \lambda_{n+}^{1,2} = \left(\frac{-b \pm i\sqrt{-\Delta}}{2} \right)^{\frac{1}{\alpha}}, \quad (28)$$

according to the sign of $\Delta = b^2 - 4c$. The stability condition for an OD state is that the real parts of all eigenvalues $\lambda_{n+}^{1,2}$ (for $n = 0, 1, 2, \dots, N/2$) are negative, which yields

$$\Lambda_{\text{COD,AOD}} = \max_{n=0,2,\dots,N/2} (\max(\text{Re}(\lambda_{n+}^{1,2}))) < 0, \quad (29)$$

where Λ_{COD} and Λ_{AOD} are the maximum real part of the eigenvalues in the case of coherent and alternating OD states, respectively. As in the case of the in-phase synchronized state, we define the following OD master stability functions: $\Lambda_{\text{COD}}(\sigma, s, \alpha)$ and $\Lambda_{\text{AOD}}(\sigma, s, \alpha)$.

3. Stability analysis: The case of coupled integer-order oscillators

Numerical simulation shows that for $\alpha \rightarrow 1$, $\Lambda_{\text{Sync}} < 0$ all through the parameter spaces of Fig. 7, which means that the in-phase synchronized state is stable throughout these parameter spaces. However, as shown in Fig. 7, the in-phase synchronized state does not cover all the parameter space in each network case. Indeed, the in-phase synchronized state coexists in certain regions of the parameter space with coherent OD and alternating OD states as shown by the results of stability analysis depicted in Fig. 10. For example, the in-phase synchronized state, coherent OD, and alternating OD states may coexist in region A. The in-phase synchronized state and alternating OD states may coexist in region B. In region C, only the in-phase synchronized state may exist. However, the realization of each of these states relies on the choice of the initial conditions¹¹ and may also rely on the interplay between the master stability functions Λ_{Sync} , Λ_{COD} , and Λ_{AOD} . Indeed, although Λ_{Sync} , Λ_{COD} , and Λ_{AOD} all have negative values in region A, comparing

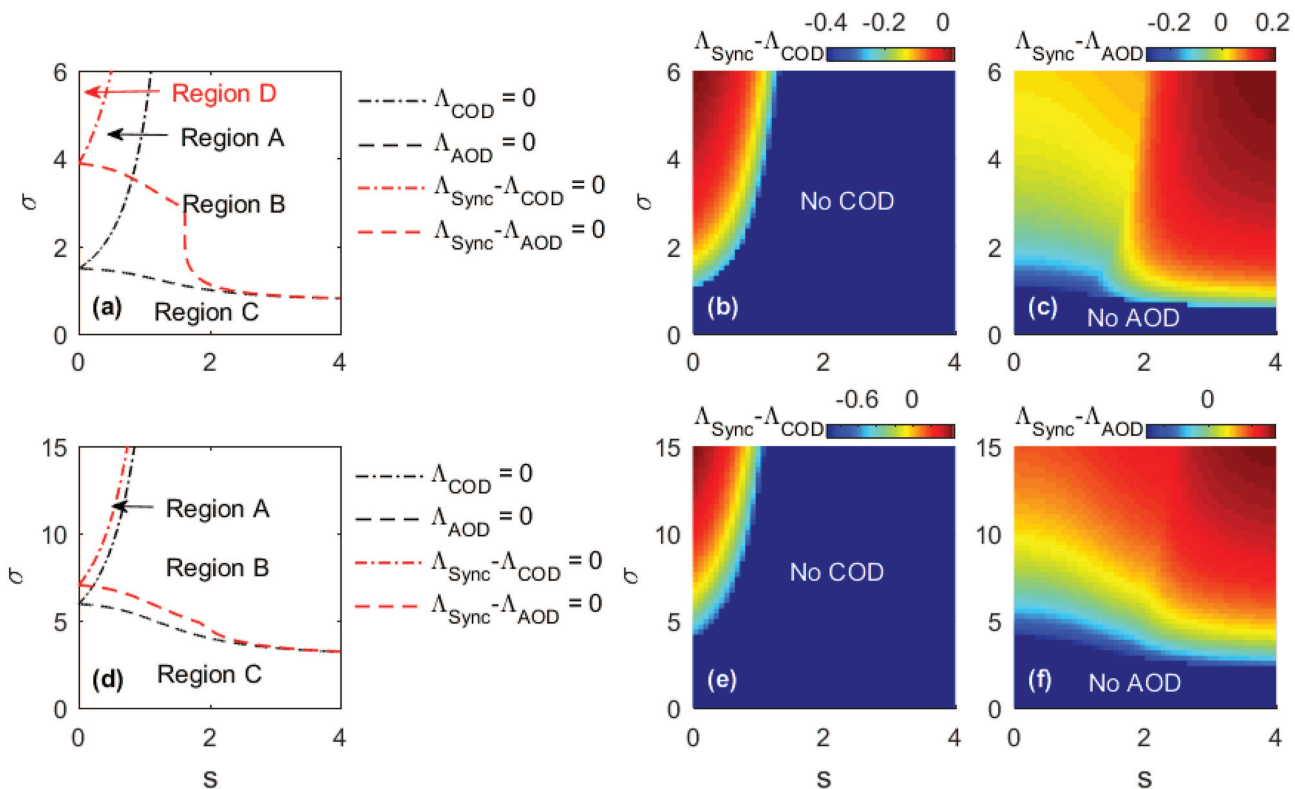


FIG. 10. Result of the stability analysis of dynamical regimes for $\alpha \rightarrow 1$ and other parameters as in Fig. 1: (a)–(c) network of van der Pol oscillators and (d)–(f) network of Rayleigh oscillators. (a) and (d) Coherent OD and alternating OD stability regions with their boundaries $\Lambda_{\text{COD}} = 0$ and $\Lambda_{\text{AOD}} = 0$ and (b), (c), (e), and (f) interplay between the master stability functions. The region above $\Lambda_{\text{COD}} = 0$ (respectively, $\Lambda_{\text{AOD}} = 0$) corresponds to stable coherent (respectively, alternating) OD states, i.e., in region A, coherent OD and alternating OD are stable, in region B, only alternating OD is stable, and in region C, all these OD states are unstable or do not exist. Note that the in-phase synchronized state is stable throughout the whole parameter space in the two networks considered as $\Lambda_{\text{Sync}}(s, \sigma) < 0$, which means that OD phenomena coexist with in-phase synchronization in regions A and B, whereas in region C, the in-phase synchronized state is the only stable state. Coherent (respectively, alternating) OD does not exist in the dark blue-colored regions in (b) and (e) [respectively, in (c) and (f)]. These phenomena may coexist with in-phase synchronization in multicolored regions, with the stability regions shown in (a) and (d).

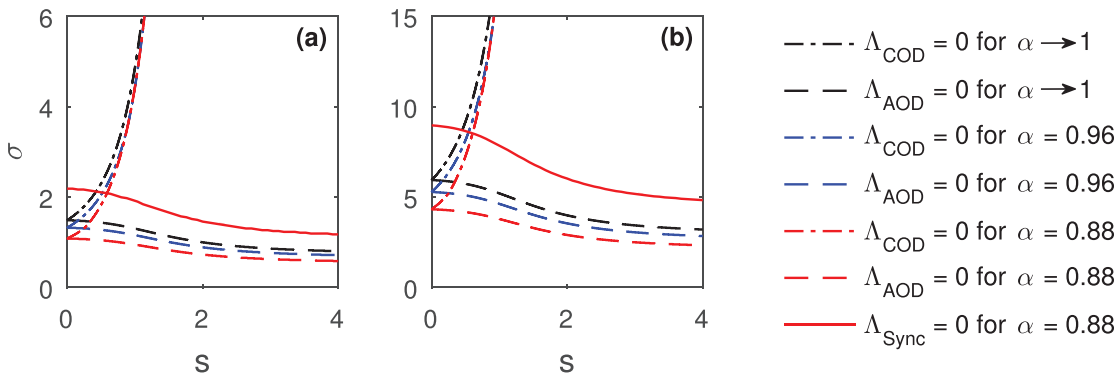


FIG. 11. Effect of fractional derivatives on the stability regions of in-phase synchronization, coherent OD, and alternating OD: (a) network of van der Pol oscillators and (b) network of Rayleigh oscillators. Coherent (respectively, alternating) OD states are stable in the region above $\Lambda_{\text{COD}} = 0$ (respectively, $\Lambda_{\text{AOD}} = 0$). The in-phase synchronized state is stable in the region below $\Lambda_{\text{Sync}} = 0$. These states do not exist or are unstable elsewhere. Note that the in-phase synchronized state is stable everywhere in the two parameter spaces for $\alpha \rightarrow 1$ and $\alpha = 0.96$. Other parameters as in Fig. 1.

the dynamical regimes in Fig. 7 and the corresponding stability diagrams in Fig. 10, one notices that the visualization of the coherent OD region in Fig. 7(c) agrees very well with the stability condition $\Lambda_{\text{COD}} < 0$ marked by region A in Fig. 10(d). This means that the initial conditions considered in this work strongly favor the occurrence of coherent OD in region A compared to in-phase synchronization and alternating OD. However, in the case of the network of van der Pol oscillators, there is a gap between region A in Fig. 10(a) and the coherent OD region in Fig. 7(a) that matches rather with region D in Fig. 10(a). Region D defined by $|\Lambda_{\text{COD}}| > |\Lambda_{\text{Sync}}|$ is a patch of region A and its complement is region \bar{D} defined by $|\Lambda_{\text{Sync}}| > |\Lambda_{\text{COD}}|$. Let us point out that the larger is the master stability function $|\Lambda|$ of a state, the earlier this state might emerge as an asymptotic state. So, as the three states mentioned above are in competition, when the distribution of initial condition is not clearly favoring one state, the state with larger dynamic master eigenvalue might take over because its probability to emerge earlier is higher. So, in the case of the van der Pol network, there is a strong competition between in-phase synchronization and coherent OD in region A that splits up in two subdomains: region D and region \bar{D} , corresponding to coherent OD and in-phase synchronization, respectively.

Still comparing Figs. 7 and 10, one can notice that alternating OD states are actually observed in stability regions defined by $\Lambda_{\text{AOD}} < 0$, i.e., region B. However, alternating OD states do not fill completely their stability regions because they coexist with the in-phase synchronized state and the distribution of initial conditions is not favorable for their realization. To understand why alternating OD emerges in the patches of region B shown in Fig. 7, we analyze the level of competition between alternating OD and in-phase synchronization. To do so, we compare Λ_{AOD} and Λ_{Sync} by visualizing $[\Lambda_{\text{Sync}}(s, \sigma) - \Lambda_{\text{AOD}}(s, \sigma)]$. The regions where alternating OD emerges in Fig. 7 match perfectly with the regions in Figs. 10(c) and 10(f) where Λ_{AOD} is larger than Λ_{Sync} , and the surface $[\Lambda_{\text{Sync}}(s, \sigma) - \Lambda_{\text{AOD}}(s, \sigma)]$ has a bump, corresponding to an explosion of the gap between Λ_{AOD} and Λ_{Sync} . These regions are visualized in Figs. 10(c) and 10(f) by dark red color.

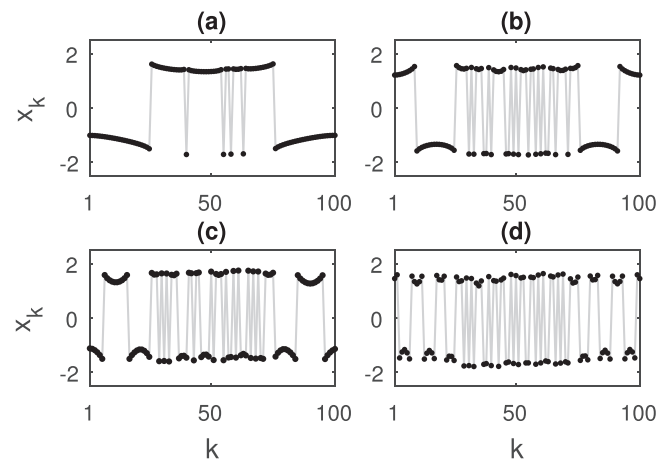


FIG. 12. Snapshots $x_k(t_{\text{snap}})$ of some partially coherent OD states exhibited by the network of fractional-order van der Pol oscillators for $\varepsilon = 4$ as in Fig. 1, $\alpha = 0.88$, $\sigma = 5.6$, and t_{snap} is any time instant taken after the transient regime. In particular, this figure shows the transitions between different OD states when the coupling exponent s varies: (a) $s = 1$: one-cluster solitary OD (1-SOD); (b) $s = 1.3$: three-cluster chimera death (3-CD); (c) $s = 1.6$: five-cluster chimera death (5-CD); and (d) $s = 2.3$: thirteen-cluster chimera death (13-CD).

Alternating OD states emerge for values of the coupling exponent s that are higher than 2, corresponding to a coupling normalization factor $\eta < 3.25$ that can be viewed as the mean number of counterparts to which each oscillator is coupled in the case of a nonlocal coupling scheme. This corresponds to a coupling range $\eta/(2N) < 0.01625$ that is favorable to the realization of amplitude chimera states.¹³ This justifies why alternating OD states are preceded by amplitude chimeras, just like the in-phase synchronized state at this scale of the coupling range.

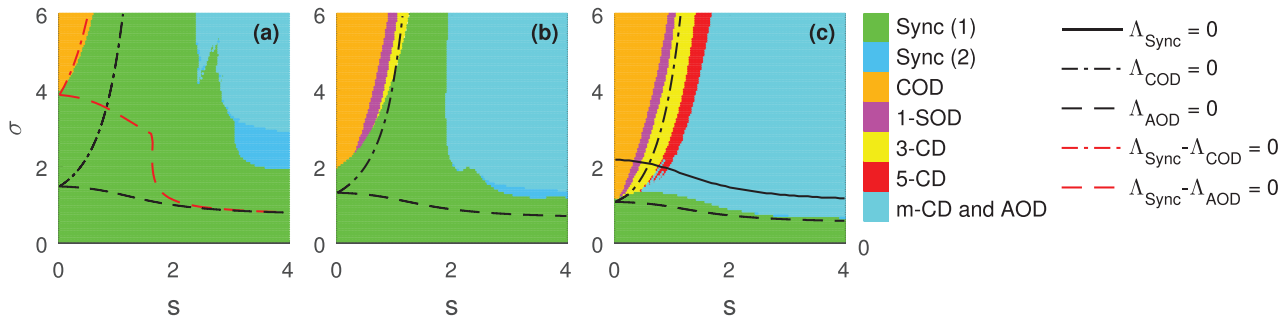


FIG. 13. Dynamical regimes of the network of van der Pol oscillators in the plane (s, σ) of coupling parameters for $\varepsilon = 4$ as in Fig. 1, and different values of the derivatives order α : (a) $\alpha \rightarrow 1$; (b) $\alpha = 0.96$; and (c) $\alpha = 0.88$. Sync: in-phase synchronization, COD: coherent oscillation death, 1-SOD: one-cluster solitary oscillation death, 3-CD: three-cluster chimera death, 5-CD: five-cluster chimera death, m -CD: multi-cluster chimera death (with $m = 7, 9, 11, \dots$), and AOD: alternating oscillation death. The in-phase synchronized state region is split up in two subdomains as in Fig. 7. In region Sync (2), the totally synchronized regime is preceded by an amplitude chimera of lifetime $t_{\text{Trans}} \geq 50T$, where T is the period of oscillation of an uncoupled integer-order van der Pol oscillator. The boundaries of dynamical regimes regions obtained from the stability analysis are superimposed on the maps.

4. Stability analysis: Fractional derivatives effect

For a fixed set (s, σ) , the master stability function $\Lambda_{\text{Sync}}(\alpha)$ increases with decreasing value of the fractional derivatives order α . Whereas on the contrary, the OD dynamic master eigenvalues $\Lambda_{\text{COD}}(\alpha)$ and $\Lambda_{\text{AOD}}(\alpha)$ decrease with increasing value of α , resulting in the expansion of the stability regions of coherent OD and alternating OD states as it is shown in Fig. 11. Overall, the simultaneous increase of $\Lambda_{\text{Sync}}(\alpha)$ and decrease of $\Lambda_{\text{COD}}(\alpha)$ and $\Lambda_{\text{AOD}}(\alpha)$ with decreasing value of α express the tendency of synchronization to disappear with decreasing value of α , for the benefit of OD states.

D. Dynamical behavior of the networks of fractional-order oscillators

The sets of equations describing the considered networks of fractional-order van der Pol and Rayleigh oscillators [Eq. (1) associated with Eqs. (3) and (4), for $\alpha > \alpha_H$] are solved with the Adams–Bashforth–Moulton predictor–corrector method with the help of the Matlab routine `FDE_PI12_PC`.⁷⁹ In this routine, the discrete convolutions (obtained by discretizing the integral in Eq. (2)) are evaluated by means of the fast Fourier transform algorithm

allowing to reduce considerably the computational cost compared to the classical implementation, while preserving the order of accuracy.⁷⁹

Apart from the collective dynamical states exhibited by the networks of integer-order van der Pol and Rayleigh oscillators (see Subsection IV A), multi-cluster chimera death states appear progressively in the networks of fractional-order oscillators as the value of the order of fractional derivatives α decreases. In particular at low values of α , if the value of the coupling strength is fixed, an increase in the coupling exponent s (i.e., a decrease in the coupling range) leads to an increase in the degree of incoherence of the death states and there is a transition from coherent two-cluster OD to totally incoherent OD states via solitary OD states and chimera death states (see Fig. 12). The number of solitary steady states in a solitary OD pattern increases with increasing value of the coupling exponent s . Thus, solitary oscillation death states represent a soft transition to incoherent oscillation death since the oscillators are leaving the coherent cluster gradually,¹¹ just like solitary states represent a soft transition to incoherent collective oscillatory behavior.⁷ In addition, it is found here that the transition from the coherent OD state to chimera death states goes through solitary OD states. In the same

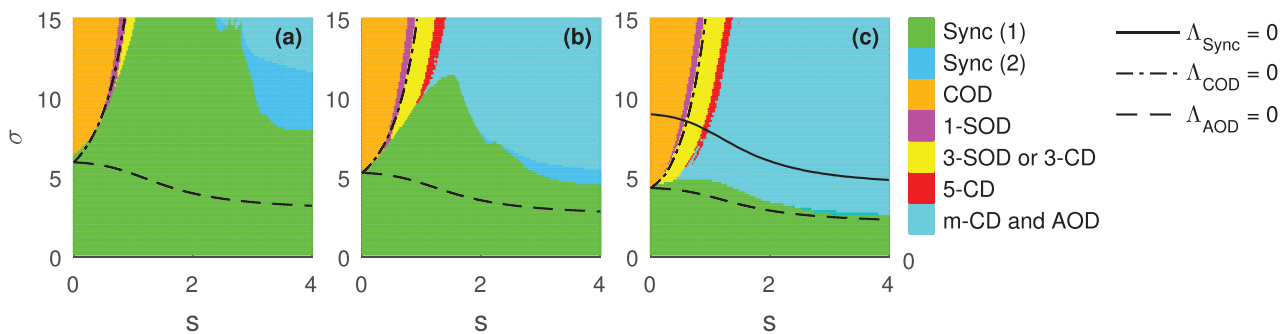


FIG. 14. Dynamical regimes of the network of Rayleigh oscillators in the plane (s, σ) of coupling parameters for $\omega = 2$ and $\mu = 1$ as in Fig. 1, and different values of the derivatives order α : (a) $\alpha \rightarrow 1$; (b) $\alpha = 0.96$; and (c) $\alpha = 0.88$. Other comments as in Fig. 13.

way, it was recently found that classical solitary states may mediate the transition from complete coherence to chimera states.^{80,81}

All these dynamical regimes are mapped in the parameter space with the help of the aforementioned characterization tools, as shown in Figs. 13 and 14. As predicted by the above stability analysis, the in-phase synchronized state disappears progressively to the benefit of multi-cluster chimera death states and alternating OD states whose degree of coherence decreases as α decreases. This also means that, for high values of the coupling exponent s , classical amplitude chimera patterns (corresponding to asymptotic in-phase synchronized state) are replaced progressively by damped amplitude chimera patterns (corresponding to asymptotic alternating OD states).

E. Fractional derivatives effect on amplitude chimeras

It was shown in Ref. 11 that the distribution of initial conditions described in the beginning of this section is not favorable to the occurrence of stable amplitude chimeras in the network of integer-order Stuart–Landau oscillators. However, it was found that under the effect of fractional derivatives, the lifetime of damped amplitude chimeras increases exponentially as the order of fractional derivatives approaches a certain critical value, suggesting the occurrence of a stable amplitude chimera at this critical value. It is worth pointing out that the lifetime of amplitude chimeras strongly depends on the initial conditions in the deterministic case.⁷⁵ The phase–antiphase (or antisymmetric) distribution of initial conditions has proved to induce stable amplitude chimeras.^{16,61,75,82} In this work, we intend to confirm the result in Ref. 11 according to which fractional derivatives can help to induce long-living, even stable amplitude chimeras with the distribution of initial conditions considered here. To do so, we analyze the effect of fractional derivatives on the amplitude chimera patterns shown in Figs. 2(b) and 3(d). Figure 15 shows that, decreasing the derivatives order α from the value 1, the classical amplitude chimera is transformed into damped amplitude chimera at a critical point noted α_C . Also, Fig. 15 shows that the lifetime t_{Trans}

of these two types of amplitude chimeras grows exponentially as the value of α comes closer to α_C . At equal distances from α_C , the lifetime of the damped amplitude chimera is extremely larger than that of the classical amplitude chimera. The exponential growth of t_{Trans} at the two sides of α_C is stopped at certain values of α very close to α_C , and one would expect a logarithmic dependence of t_{Trans} with respect to α in the exponentially narrow interval of α around α_C , as it is the case for $t_{\text{Trans}}(\sigma)$ in Fig. 8.

V. CONCLUSION

In this paper, we have explored the impact of fractional derivatives on the symmetry-breaking dynamics of coupled systems of identical limit-cycle oscillators. In a previous work,¹¹ it was found that a decrease in the derivatives order induces significant qualitative and quantitative changes in the symmetry-breaking dynamical behavior of a network of fractional-order Stuart–Landau oscillators. In the present work, we have considered two important limit-cycle oscillators, namely, the van der Pol and Rayleigh oscillators. The coupled systems of these two oscillator models are capable, as coupled Stuart–Landau oscillators, to exhibit amplitude chimeras and oscillation death phenomena. It was previously found that coupled systems of Rayleigh oscillators can exhibit amplitude chimera states, but their occurrence in a network of van der Pol oscillators has not been observed yet. Studying networks of fractional-order versions of these two limit-cycle oscillators, we have demonstrated that the results of the aforementioned previous work can be generalized. At first, the coupled dynamics of integer-order oscillators has been explored thoroughly. And, it has been found that the two coupled systems can exhibit two types of amplitude chimeras, namely, the classical amplitude chimera (transient to an in-phase synchronized state) and a novel amplitude chimera state named here “damped amplitude chimera,” whose (i) incoherent region(s) size increases continuously in the course of time and (ii) drifting units oscillations are damped continuously until they are quenched. Besides these transient regimes with oscillatory behaviors, some simple oscillation death states emerge in the behavior of the two networks. In particular, we have observed solitary oscillation death states in the behavior of the network of Rayleigh oscillators. Then, the effect of fractional derivatives has been investigated, which reveals that multi-cluster chimera death states are induced in the networks’ dynamics by the fractional derivatives. Under the effect of fractional derivatives, the classical amplitude chimera is transformed into damped amplitude chimera. Indeed, as the value of the fractional derivatives order decreases, the lifetime of classical amplitude chimeras increases, and there is a critical point at which there is a transition to damped amplitude chimeras. In addition, damped amplitude chimera patterns become gradually short-living transient states, which expresses the tendency of the coupled systems to stabilization toward steady states under the effect of fractional derivatives. Overall, a decrease in the order of fractional derivatives reduces the networks’ ability to synchronization and promotes diverse oscillation death patterns. The results have been verified by the stability analysis of synchronization and of some oscillation death states carried out with the help of the properties of the dynamic eigenvalues associated with the block-diagonalized variational equations of the coupled systems.

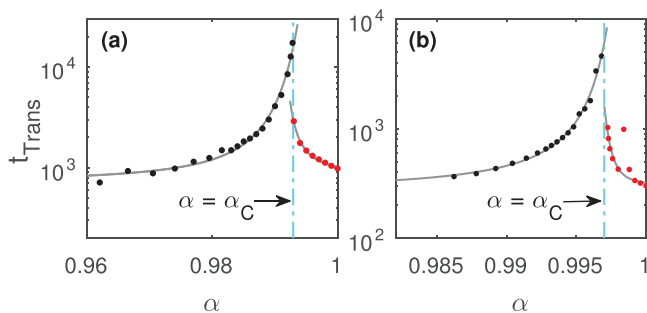


FIG. 15. Amplitude chimeras lifetime t_{Trans} (in logarithmic scale) vs fractional derivatives order α : (a) network of fractional-order van der Pol oscillators with the parameters of Fig. 2(b) and (b) network of fractional-order Rayleigh oscillators with the parameters of Fig. 3(d). Red (respectively, black) dots for classical (respectively, damped) amplitude chimeras. The gray lines are fitting curves obtained with the formula $t_{\text{Trans}}(\alpha) = b \exp(c/(\alpha - e)) + d$, where b, c, d , and e are different sets of fit parameters for each curve.

The present study will deepen our understanding of the emergent dynamics of coupled fractional-order systems.

ACKNOWLEDGMENTS

S. G. Ngueuteu Mbouna would like to acknowledge Professor Roberto Garrappa (Department of Mathematics, University of Bari) for having kindly provided him with the literature on the Matlab routine FDE_PI12_PC.

AUTHOR DECLARATIONS

Conflict of Interest

The authors have no conflicts to disclose.

Author Contributions

S. G. Ngueuteu Mbouna: Conceptualization (equal); Formal analysis (equal); Investigation (equal); Methodology (equal); Software (equal); Writing – original draft (equal). **Tannoy Banerjee:** Conceptualization (equal); Supervision (equal); Writing – review & editing (equal). **Eckehard Schöll:** Conceptualization (equal); Supervision (equal); Writing – review & editing (equal). **René Yamapi:** Conceptualization (equal); Supervision (equal); Writing – review & editing (equal).

DATA AVAILABILITY

The data that support the findings of this study are available within the article.

REFERENCES

- ¹A. Pikovsky, M. Rosenblum, and J. Kurths, *Synchronization: A Universal Concept in Nonlinear Science* (Cambridge University Press, Cambridge, 2001).
- ²A. Balanov, N. Janson, D. Postnov, and O. Sosnovtseva, *Synchronization: From Simple to Complex* (Springer-Verlag, Berlin, 2009).
- ³S. Strogatz, *Sync: The Emerging Science of Spontaneous Order* (Hyperion, New York, 2003).
- ⁴S. Boccaletti, A. N. Pisarchik, C. I. del Genio, and A. Amann, *Synchronization: From Coupled Systems to Complex Networks* (Cambridge University Press, Cambridge, 2018).
- ⁵Y. Kuramoto and D. Battogtokh, *Nonlinear Phenom. Complex Syst.* **5**, 380 (2002).
- ⁶D. M. Abrams and S. H. Strogatz, *Phys. Rev. Lett.* **93**, 174102 (2004).
- ⁷A. Zakharova, *Chimera Patterns in Networks: Interplay between Dynamics, Structure, Noise, and Delay* (Springer Nature Switzerland AG, Cham, 2020).
- ⁸F. Parastesh, S. Jafari, H. Azarnoush, Z. Shahriari, Z. Wang, S. Boccaletti, and M. Perc, *Phys. Rep.* **898**, 1 (2021).
- ⁹A. Koseska, E. Volkov, and J. Kurths, *Phys. Rep.* **531**, 173 (2013).
- ¹⁰W. Zou, D. V. Senthilkumar, M. Zhan, and J. Kurths, *Phys. Rep.* **931**, 1 (2021).
- ¹¹S. G. Ngueuteu Mbouna, T. Banerjee, R. Yamapi, and P. Wofo, *Chaos Solitons Fract.* **157**, 111945 (2022).
- ¹²I. Schneider, M. Kapeller, S. Loos, A. Zakharova, B. Fiedler, and E. Schöll, *Phys. Rev. E* **92**, 052915 (2015).
- ¹³A. Zakharova, M. Kapeller, and E. Schöll, *Phys. Rev. Lett.* **112**, 154101 (2014).
- ¹⁴I. Omelchenko, A. Zakharova, P. Hövel, J. Siebert, and E. Schöll, *Chaos* **25**, 083104 (2015).
- ¹⁵T. Banerjee and D. Ghosh, *Phys. Rev. E* **89**, 062902 (2014).
- ¹⁶B. Bandyopadhyay, T. Khatun, P. S. Dutta, and T. Banerjee, *Chaos Solitons Fract.* **139**, 110289 (2020).
- ¹⁷A. Rontogiannis and A. Provata, *Eur. Phys. J. B* **94**, 97 (2021).
- ¹⁸S. G. Ngueuteu Mbouna, T. Banerjee, and E. Schöll, *Phys. Rev. E* **107**, 054204 (2023).
- ¹⁹T. Banerjee, P. S. Dutta, A. Zakharova, and E. Schöll, *Phys. Rev. E* **94**, 032206 (2016).
- ²⁰R. Caponetto, R. Dongola, L. Fortuna, and I. Petráš, *Fractional Order Systems: Modeling and Control Applications* (World Scientific Publishing Co. Pte. Ltd., Singapore, 2010).
- ²¹R. C. Koeller, *J. Appl. Mech.* **51**, 299 (1984).
- ²²F. Mainardi, *Fractional Calculus and Waves in Linear Viscoelasticity: An Introduction to Mathematical Models* (Imperial College Press, London, 2010).
- ²³*Fractional Dynamics: Recent Advances*, edited by J. Klafter, S. C. Lim, and R. Metzler (World Scientific Publishing Co. Pte. Ltd., Singapore, 2012).
- ²⁴S. Westerlund and I. Ekstam, *IEEE Trans. Dielectr. Electr. Insul.* **1**, 826 (1994).
- ²⁵S. Westerlund, *Dead Matter Has Memory!* (Causal Consulting, Kalmar, 2002).
- ²⁶S. Faraji and M. S. Tavazoei, *Cent. Eur. J. Phys.* **11**, 836 (2013).
- ²⁷I. Schäfer and K. Krüger, *J. Phys. D: Appl. Phys.* **41**, 045001 (2008).
- ²⁸R. L. Magin, *Fractional Calculus in Bioengineering* (Begell House, CT, 2006).
- ²⁹R. L. Magin, *Comput. Math. Appl.* **59**, 1586 (2010).
- ³⁰B. N. Lundstrom, M. H. Higgs, W. J. Spain, and A. L. Fairhall, *Nat. Neurosci.* **11**, 1335 (2008).
- ³¹W. Tekla, T. M. Marinov, and F. Santamaria, *PLOS Comput. Biol.* **10**, e1003526 (2014).
- ³²I. Goychuk and P. Hänggi, *Phys. Rev. E* **70**, 051915 (2004).
- ³³S. Z. Rida, A. M. A. El-Sayed, and A. A. M. Arafa, *J. Stat. Phys.* **140**, 797 (2010).
- ³⁴C. Ionescu, A. Lopes, D. Copot, J. A. T. Machado, and J. H. T. Bates, *Commun. Nonlinear Sci. Numer. Simulat.* **51**, 141 (2017).
- ³⁵C. li, X. Liao, and J. Yu, *Phys. Rev. E* **68**, 067203 (2003).
- ³⁶W. Deng, *Phys. Rev. E* **75**, 056201 (2007).
- ³⁷G. S. M. Ngueuteu and P. Wofo, *Mech. Res. Commun.* **46**, 20 (2012).
- ³⁸I. Petráš, *Fractional-Order Nonlinear Systems: Modeling, Analysis and Simulation* (Higher Education Press, Beijing, 2011).
- ³⁹F. Zhang, G. Chen, C. Li, and J. Kurths, *Philos. Trans. R. Soc. A* **371**, 20120155 (2013).
- ⁴⁰*Fractional Order Control and Synchronization of Chaotic Systems*, edited by A. T. Azar, S. Vaidyanathan, and A. Ouannas (Springer International Publishing AG, Cham, 2017).
- ⁴¹G. S. M. Ngueuteu, R. Yamapi, and P. Wofo, *Europhys. Lett.* **112**, 30004 (2015).
- ⁴²Q. X. Liu, J. K. Liu, and Y. M. Chen, *Commun. Nonlinear Sci. Numer. Simulat.* **48**, 414 (2017).
- ⁴³Z. Sun, R. Xiao, X. Yang, and W. Xu, *Chaos* **28**, 033109 (2018).
- ⁴⁴R. Xiao, Z. Sun, X. Yang, and W. Xu, *Commun. Nonlinear Sci. Numer. Simulat.* **69**, 168 (2019).
- ⁴⁵S. Liu, Z. Sun, and N. Zhao, *Chaos* **30**, 103108 (2020).
- ⁴⁶Y. Liu, Z. Sun, X. Yang, and W. Xu, *Commun. Nonlinear Sci. Numer. Simulat.* **93**, 105501 (2021).
- ⁴⁷P. Vázquez-Guerrero, J. F. Gómez-Aguilar, F. Santamaria, and R. F. Escobar-Jiménez, *Physica A* **539**, 122896 (2020).
- ⁴⁸S. He, *Front. Appl. Math. Stat.* **6**, 24 (2020).
- ⁴⁹D. Ghosh, T. Banerjee, and J. Kurths, *Phys. Rev. E* **92**, 052908 (2015).
- ⁵⁰K. Kumar, D. Biswas, T. Banerjee, W. Zou, J. Kurths, and D. V. Senthilkumar, *Phys. Rev. E* **100**, 052212 (2019).
- ⁵¹N. Zhao, Z. Sun, X. Yang, and W. Xu, *Phys. Rev. E* **97**, 062203 (2018).
- ⁵²A. Franci, M. A. Herrera-Valdez, M. Lara-Aparicio, and P. Padilla-Longoria, *Front. Appl. Math. Stat.* **4**, 51 (2018).
- ⁵³S. Dixit, A. Sharma, and M. D. Shrimali, *Phys. Lett. A* **383**, 125930 (2019).
- ⁵⁴V. M. Bastidas, I. Omelchenko, A. Zakharova, E. Schöll, and T. Brandes, *Phys. Rev. E* **92**, 062924 (2015).
- ⁵⁵C. R. Hens, A. Mishra, P. K. Roy, A. Sen, and S. K. Dana, *Pramana* **84**, 229 (2015).
- ⁵⁶S. Ulonska, I. Omelchenko, A. Zakharova, and E. Schöll, *Chaos* **26**, 094825 (2016).
- ⁵⁷J. Sawicki, I. Omelchenko, A. Zakharova, and E. Schöll, *Eur. Phys. J. Spec. Top.* **226**, 1883 (2017).
- ⁵⁸M. Desroches and M. R. Jeffrey, *Proc. R. Soc. A* **467**, 2404 (2011).

- ⁵⁹D. Kaplan and L. Glass, *Understanding Nonlinear Dynamics* (Springer-Verlag, New York, 1995).
- ⁶⁰T. Kanamaru, *Scholarpedia* **2**, 2202 (2007).
- ⁶¹T. Banerjee, D. Biswas, D. Ghosh, E. Schöll, and A. Zakharova, *Chaos* **28**, 113124 (2018).
- ⁶²S. E. de S. Pinto, S. R. Lopes, and R. L. Viana, *Physica A* **303**, 339 (2002).
- ⁶³A. M. dos Santos, C. F. Woellner, S. R. Lopes, A. M. Batista, and R. L. Viana, *Chaos Solitons Fract.* **32**, 702 (2007).
- ⁶⁴C. Li and W. Deng, *Appl. Math. Comput.* **187**, 777 (2007).
- ⁶⁵L. Rayleigh, *Lond. Edinb. Dublin Philos. Mag. J. Sci.* **15**, 229 (1883).
- ⁶⁶R. FitzHugh, *Biophys. J.* **1**, 445 (1961).
- ⁶⁷J. Nagumo, S. Arimoto, and S. Yoshizawa, *Proc. IRE* **50**, 2061 (1962).
- ⁶⁸M. S. Tavazoei and M. Haeri, *Automatica* **45**, 1886 (2009).
- ⁶⁹H. R. Henriquez, M. Pierrri, and P. Taboas, *J. Math. Anal. Appl.* **343**, 1119 (2008).
- ⁷⁰R. Garrappa, E. Kaslik, and M. Popolizio, *Mathematics* **7**, 407 (2019).
- ⁷¹M.-S. Abdelouahab, R. Lozi, and G. Chen, *Int. J. Bifurcat. Chaos* **29**, 1950111 (2019).
- ⁷²K. Diethelm, N. J. Ford, and A. D. Freed, *Nonlinear Dyn.* **29**, 3 (2002).
- ⁷³C. Li, A. Chen, and J. Ye, *J. Comput. Phys.* **230**, 3352 (2011).
- ⁷⁴I. Omelchenko, O. E. Omel'chenko, P. Hövel, and E. Schöll, *Phys. Rev. Lett.* **110**, 224101 (2013).
- ⁷⁵L. Tumash, A. Zakharova, J. Lehnert, W. Just, and E. Schöll, *Europhys. Lett.* **117**, 20001 (2017).
- ⁷⁶S. A. M. Loos, J. C. Claussen, E. Schöll, and A. Zakharova, *Phys. Rev. E* **93**, 012209 (2016).
- ⁷⁷J. F. Heagy, T. L. Carroll, and L. M. Pecora, *Phys. Rev. E* **50**, 1874 (1994).
- ⁷⁸L. M. Pecora and T. L. Carroll, *Phys. Rev. Lett.* **80**, 2109 (1998).
- ⁷⁹R. Garrappa, *Mathematics* **6**, 16 (2018).
- ⁸⁰P. Jaros, Y. Maistrenko, and T. Kapitaniak, *Phys. Rev. E* **91**, 022907 (2015).
- ⁸¹L. Schülen, A. Gerdes, M. Wolfrum, and A. Zakharova, *Phys. Rev. E* **106**, L042203 (2022).
- ⁸²K. Sathiyadevi, V. K. Chandrasekar, and D. V. Senthilkumar, *Phys. Rev. E* **98**, 032301 (2018).